Acta Cryst C STRUCTURAL CHEMISTRY

ISSN 2053-2296

Effect of the size of halide ligands on the crystal structures of halide-bibridged polymers of HgX_2 with 4-ethylpyridine

B. M. Parveen Beebeejaun-Boodoo*

Department of Chemistry, University of Pretoria, Private Bag X20, Hatfield, 0028, Pretoria, South Africa. *Correspondence e-mail: parveen.beebeejaun@up.ac.za

Received 10 April 2025
Accepted 1 November 2025

Edited by E. Reinheimer, Rigaku Americas Corporation, USA

Keywords: coordination polymers; crystal structure; halide-bibridged polymers; mercury; ethylpyridine; organic-inorganic hybrid.

CCDC references: 2442692; 2442693; 2442694

Supporting information: this article has supporting information at journals.iucr.org/c

Halide-bridged polymers are a type of coordination polymer whereby halide ligands act as bridging ligands between the metal centres. The crystal structures of three halide-bibridged polymers of the formula $[Hg(\mu\text{-}X)_2(4\text{-Etpy})]_n$, namely, *catena*-poly[[(4-ethylpyridine)mercury(II)]-di-μ-halido], obtained through the combination of the organic ligand 4-ethylpyridine (4-Etpy, C_7H_9N) and HgX_2 (X = Cl, Br or I), were determined. In these structures, abbreviated as **4epHgCl**, **4epHgBr** and **4epHgI**, respectively, the Hg^{II} ion exhibits a coordination number of five. All three structures were found to display a similar one-dimensional scalloped polymeric chain with halide ligands bridging pairs of Hg^{II} ions in a bidentate fashion; however, **4epHgI** differs from the other two structures in terms of the packing arrangement of the polymer. The change of the halide ligand to the larger iodide ligand disrupts the formation of the regular halide-bibridged polymeric chain observed in the chloride and bromide analogues, with **4epHgI** displaying pseudo-bridging in the polymer chain.

1. Introduction

Halide-bridged polymers are a subgroup of coordination compounds comprising metal ions that are linked *via* bridging halide ligands into a polymeric structure. The metal ions are typically also coordinated to additional organic ligands, resulting in a polymer of the formula $[M(\mu\text{-}X)_y(L)_z]_n$, with M indicating the metal ion, X the bridging halide ligand and L the organic ligand. Additional terminal halide ligands may also be present in these polymers. The structural diversity displayed by halide-bridged polymers make them excellent candidates for use in crystal engineering studies.

Halide-bridged polymers display physical properties, such as magnetic exchange and electrical conductivity along the halide-bridged polymer, as well as luminescence, catalytic activity and non-linear optical properties (Givaja *et al.*, 2012; Eckberg *et al.*, 1975; Crawford *et al.*, 1977; Estes *et al.*, 1978; Zhang *et al.*, 1997; Wei *et al.*, 1996; Slabbert *et al.*, 2015*a*). Of specific interest in the current study are halide-bridged polymers containing the metal ion Hg^{II} and the organic ligand 4-ethylpyridine (4-Etpy).

The Hg^{II} ion shows a range of coordination configurations ranging from trigonal planar, square-planar and octahedral to the preferred tetrahedral environment due to its softness and fully filled orbitals, allowing it to bind with soft anions such as Cl^-, Br^- and I^- (Slabbert *et al.*, 2015*b*; Englert *et al.*, 2010; Hu *et al.*, 2007). The coordination around the Hg^{II} cations allows for a wide range of bonding distances to potential donor atoms (Englert *et al.*, 2010). Halide-bridged polymers of divalent d^{10} metal cations with N-donor ligands have been studied,

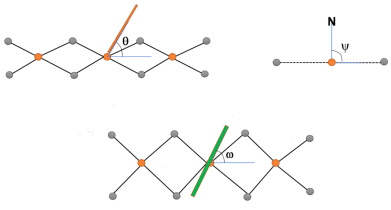

focusing on the effect of electronically modified pyridine/pyrazine-derived N-donor ligands on the structure of the coordinated halide-bridged chain (Hu *et al.*, 2001, 2003; Wang *et al.*, 2009; Mahmoudi *et al.*, 2009; Morsali *et al.*, 2009). The size of the N-donor organic ligand has an effect on the halide-bridged polymer and the extent to which the width of the coordinating N-donor organic ligand can be increased without disrupting the chain of the halide-bridged polymer has also been investigated (Slabbert *et al.*, 2015*b*).

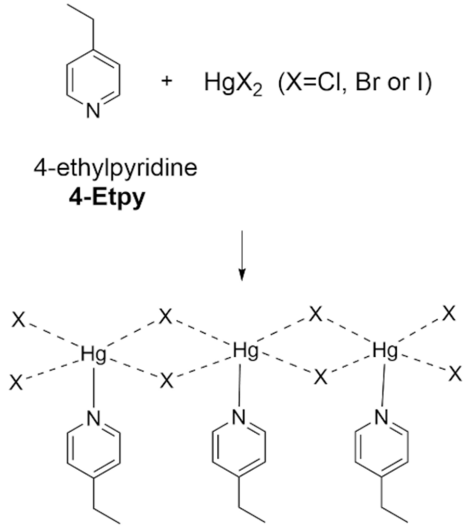

4epHgCl: [Hg(μ-Cl)$_2$(4-Etpy)]
4epHgBr: [Hg(μ-Br)$_2$(4-Etpy)]
4epHgI: [Hg(μ-I)$_2$(4-Etpy)]

Scheme 1

A one-dimensional polymeric structure with composition $[Hg(\mu\text{-}Cl)_2(pyridine)_2]_n$ was reported for the combination of pyridine with $HgCl_2$, and the structure obtained is a chloride-bridged polymeric lattice of $HgCl_4$ square-planar entities with pyridine ligands occupying the *trans*-octahedral sites around the Hg^{II} ion (Canty *et al.*, 1982). However, when the halide was changed from Cl^- to Br^- and I^-, no polymer was formed. The reactions of HgX_2 (X = Cl, Br or I) with the organic ligand 2-(2-hydroxyethyl)pyridine also formed one-dimensional polymeric chains of $[(X)Hg(\mu\text{-}X)_2\{2\text{-}(2\text{-hydroxyethyl})pyridine\}]_n$ (Mobin *et al.*, 2010). In these polymers, the organic ligand binds to the Hg^{II} ion in a monotopic fashion *via* only the pyridine N-atom donor, leaving the $-(CH_2)_2OH$ group at the *ortho* position as a pendant ligand. The halide-bridged polymer can either adopt a planar or a zigzag motif due to the flexibility of the Hg^{II} metal centre. If the bridging halide ligands of adjacent Hg^{II} ions are not arranged in a coplanar fashion, then a zigzag structure is favoured (Englert *et al.*, 2010).

A search of the Cambridge Structural Database (CSD, Version 5.46, February 2025 update; Groom *et al.*, 2016) revealed that no crystal structure containing the organic ligand 4-ethylpyridine and Hg^{II} has been reported in the literature. This indicated a gap in the literature, prompting the current investigation. This present study focuses on the organic–inorganic hybrid compounds formed by the reaction of HgX_2 (X = Cl, Br or I) with the N-donor ligand 4-ethylpyridine (4-Etpy), as illustrated in Scheme 1. The structures of the compounds formed are abbreviated as **4epHg*X***, with **4ep** representing the organic ligand and **Hg*X*** referring to the halide-bridged portion of the polymer. These reactions resulted in the formation of three new one-dimensional halide-bibridged polymers, namely, *catena*-poly[[(4-ethylpyridine)mercury(II)]-di-μ-chlorido], **4epHgCl**, *catena*-poly[[(4-ethylpyridine)mercury(II)]-di-μ-bromido], **4epHgBr**, and *catena*-poly[[(4-ethylpyridine)mercury(II)]-di-μ-iodido], **4epHgI**.

2. Experimental

2.1. Chemicals and reagents

All chemicals were used as purchased without further purification: $HgCl_2$ (98%, Fluka), $HgBr_2$ (98%, Sigma–Aldrich), HgI_2 (99%, Riedel de Haen), 4-ethylpyridine (98%, Sigma–Aldrich), ethanol (EtOH) (99.5%, Merck), methanol (MeOH) (99%, Merck) and tetrahydrofuran (THF) (99.9%, Sigma–Aldrich).

2.2. Synthesis and crystallization

2.2.1. Synthesis of 4epHgCl

A solution of $HgCl_2$ (0.954 mmol, 0.2589 g) dissolved in EtOH (5 ml) was added to a slightly heated and stirred solution of 4-ethylpyridine (0.961 mmol, 0.1030 g) dissolved in EtOH (10 ml). The resulting solution was heated for 15 min and left at room temperature, open to the atmosphere, to crystallize. A batch of colourless rod-like crystals of **4epHgCl** were harvested (yield 57%) upon formation after two weeks.

2.2.2. Synthesis of 4epHgBr

A solution of $HgBr_2$ (0.933 mmol, 0.3363 g) dissolved in THF (7 ml) was added to a slightly heated and stirred solution of 4-ethylpyridine (0.944 mmol, 0.1012 g) dissolved in MeOH (10 ml). The resulting solution was heated for 15 min, covered with Parafilm and left to crystallize at room temperature. A batch of colourless rod-like crystals of **4epHgBr** were harvested (yield 62%) upon formation after two weeks.

2.2.3. Synthesis of 4epHgI

A solution of HgI_2 (0.940 mmol, 0.4270 g) dissolved in THF (7 ml) was added to a slightly heated and stirred solution of 4-ethylpyridine (0.950 mmol, 0.1018 g) dissolved in MeOH (10 ml). The resulting solution was heated for 15 min, covered with Parafilm and left to crystallize at room temperature. A batch of colourless needle-like crystals of **4epHgI** were harvested (yield 59%) upon formation after two weeks.

2.3. Refinement

Crystal data, data collection and structure refinement details are summarized in Table 1. The structures of **4epHgCl** and **4epHgI** were refined as two-component inversion twins

Table 1
Experimental details.

Experiments were carried out at 150 K with Mo $K\alpha$ radiation using a Bruker PHOTON 100 CMOS diffractometer. Absorption was corrected for by multi-scan methods (*SADABS*; Bruker, 2013). H-atom parameters were constrained.

	4epHgCl	**4epHgBr**	**4epHgI**
Crystal data			
Chemical formula	$[HgCl_2(C_7H_9N)]$	$[HgBr_2(C_7H_9N)]$	$[HgI_2(C_7H_9N)]$
M_r	378.64	467.54	561.54
Crystal system, space group	Orthorhombic, $P2_12_12_1$	Monoclinic, $P2_1/c$	Orthorhombic, $Fdd2$
a, b, c (Å)	3.9382 (5), 10.3571 (15), 22.758 (3)	4.0679 (5), 22.583 (3), 10.9050 (14)	30.3836 (14), 34.6159 (16), 4.3247 (2)
α, β, γ (°)	90, 90, 90	90, 95.488 (4), 90	90, 90, 90
V (Å^3)	928.3 (2)	997.2 (2)	4548.5 (4)
Z	4	4	16
μ (mm^{-1})	17.09	23.39	18.91
Crystal size (mm)	0.51 × 0.23 × 0.12	0.42 × 0.18 × 0.10	0.23 × 0.06 × 0.06
Data collection			
T_{min}, T_{max}	0.068, 0.260	0.244, 0.745	0.366, 0.747
No. of measured, independent and observed [$I > 2\sigma(I)$] reflections	16644, 1876, 1869	21065, 2024, 1908	30677, 2271, 2251
R_{int}	0.058	0.062	0.038
$(\sin\theta/\lambda)_{max}$ (Å^{-1})	0.625	0.625	0.625
Refinement			
$R[F^2 > 2\sigma(F^2)]$, $wR(F^2)$, S	0.020, 0.053, 1.11	0.033, 0.094, 1.08	0.018, 0.045, 1.15
No. of reflections	1876	2024	2271
No. of parameters	103	96	102
No. of restraints	0	0	1
H-atom treatment	H-atom parameters constrained	H-atom parameters constrained	H-atom parameters constrained
$\Delta\rho_{max}$, $\Delta\rho_{min}$ (e Å^{-3})	1.29, −1.22	2.19, −1.85	1.17, −0.46
Absolute structure	Refined as an inversion twin	–	Refined as an inversion twin
Absolute structure parameter	0.186 (14)	–	0.026 (7)

Computer programs: *APEX2* (Bruker, 2013), *SAINT* (Bruker, 2013), *SHELXT2013* (Sheldrick, 2015*a*) and *SHELXL2013* (Sheldrick, 2015*b*) in *WinGX* (Farrugia, 2012), *Mercury* (Macrae *et al.*, 2020), *PLATON* (Spek, 2020) and *OLEX2* (Dolomanov *et al.*, 2009).

with the twin law ($\bar{1}00\ 0\bar{1}0\ 00\bar{1}$) applied to both. The BASF was refined to 0.186 for **4epHgCl** and 0.026 for **4epHgI**. The inclusion of the twin refinement improved the quality of the models, as evidenced by a decrease in the *R* factor. The riding model was employed to position the H atoms in the three structures.

3. Results and discussion

3.1. Crystallographic discussion of the structures

Three new crystal structures containing 4-ethylpyridine (4-Etpy) with Hg^{II} halides as the inorganic portions were determined, all displaying one-dimensional halide-bibridged polymeric structures, in which the Hg^{II} cations are bridged by two halide ligands. The crystallographic parameters of these structures are listed in Table 1 and their asymmetric units are illustrated in Fig. 1. Selected bond lengths and bond angles are given in Table S1 and weak C—H···*X* hydrogen-bonding interactions in Table S2 in the supporting information.

3.2. Crystal structures of 4epHgCl, 4epHgBr and 4epHgI

Similar one-dimensional halide-bridged polymers were obtained for **4epHgCl**, **4epHgBr** and **4epHgI**; however, they are not isostructural. **4epHgCl**, **4epHgBr** and **4epHgI** crystallize in the space groups $P2_12_12_1$, $P2_1/c$ and $Fdd2$, respectively. The asymmetric units of all three structures consist of a Hg^{II} ion coordinated to two halide ligands and one 4-ethylpyridine organic ligand coordinated *via* the N atom, as illustrated in Fig. 1.

Repetition of the asymmetric unit results in the formation of a one-dimensional halide-bibridged polymer in all three structures, in which pairs of Hg^{II} ions are bridged by two halide ligands, as illustrated in Figs. 2(*a*)–(*c*). The polymer adopts a scalloped ribbon conformation, with all the organic ligands coordinated to the same side of the polymer chain, as shown in Figs. 2(*d*)–(*f*). In these polymers, the Hg^{II} ion adopts a square-pyramidal geometry, with four equatorial halide ligands and the 4-ethylpyridine ligand as the axial ligand. It was found that the basal plane of the square pyramid is not coplanar with the Hg^{II} ion in all three structures, indicating a slight distortion in the geometry.

In all the structures, the metal halide portion displays a puckered pseudo-parallelogram geometry, consisting of four unequal Hg—*X* bonds, in which the two opposite Hg—*X* bond lengths are similar, with two Hg—*X* bonds being shorter and two longer. Shorter Hg—*X* bonds alternate with longer Hg—*X* bonds, with similar shorter Hg—*X* bond lengths of 2.3471 (18) and 2.3562 (18) Å in **4epHgCl**, 2.4732 (8) and 2.4815 (8) Å in **4epHgBr**, and 2.6269 (6) and 2.6576 (6) Å in **4epHgI**. The polymer chain in **4epHgI** adopts a similar pattern to that of **4epHgCl and 4epHgBr**, but does not consist of the repeating pseudo-parallelogram motif, but rather features open pseudo-parallelogram units, as illustrated in Fig. 2(*f*).

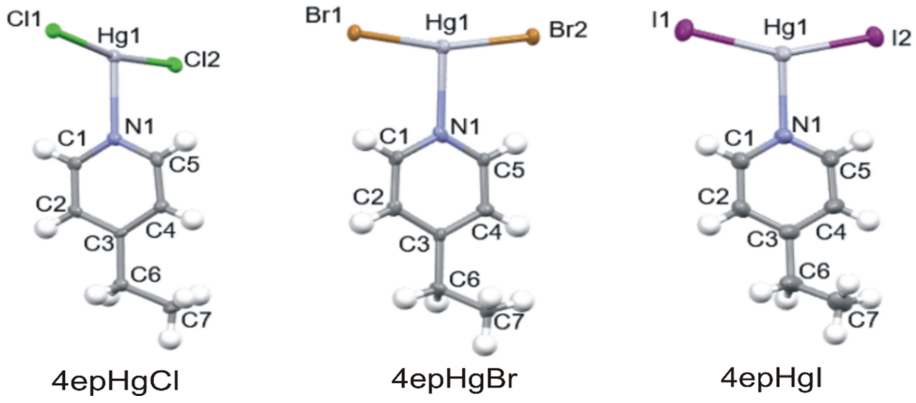

Figure 1
The asymmetric units of **4epHgCl**, **4epHgBr** and **4epHgI**, showing the atomic numbering schemes. Displacement ellipsoids are drawn at the 50% probability level for all the structures and H atoms are shown as small spheres of arbitrary radii.

The longer Hg—*X* bonds may be viewed as semi-coordinated interactions, and have values of 3.086 (2) and 3.094 (2) Å in the chloride structure, 3.1704 (9) and 3.2694 (2) Å in the bromide structure, and 3.1949 (6) and 3.8988 (8) Å in the iodide structure. The presence of the very long semi-coordinated Hg—I bond of 3.8988 (8) Å in **4epHgI** causes the iodide-bibridged polymer to have a distorted geometry compared to the polymers in **4epHgCl** and **4epHgBr**, as can be seen in Figs. 2(*d*)–(*f*) (Slabbert *et al.*, 2015*b*). The puckered geometry of the halide-bridged polymers in related compounds has been reported previously and is a mechanism to shorten the Hg···Hg distance, and thus the distance between the aromatic planes of the organic ligands, to allow for the formation of aromatic interactions between the organic ligands (Slabbert *et al.*, 2015*b*).

As the size of the halide ligand increases from chloride to bromide to iodide, the Hg—*X* bond lengths increase, resulting in an increase in the Hg···Hg distance in the halide-bibridged polymer. The Hg···Hg distance is 3.9382 (6) Å in **4epHgCl**, 4.0679 (6) Å in **4epHgBr** and 4.3247 (5) Å in **4epHgI**, indicating very weak mercurophilic interactions (Kumar *et al.*, 2013; Doerrer *et al.*, 2010) in the polymer chain. The Hg—N bond lengths decrease with an increase in halide ligand size, with Hg—N bond lengths of 2.441 (6) Å in **4epHgCl**, 2.436 (7) Å in **4epHgBr** and 2.373 (7) Å in **4epHgI**.

Along the halide-bibridged polymer, the two opposite angles *X*1—Hg—*X*1 and *X*2—Hg—*X*2 have larger values than the *X*1—Hg—*X*2 angles within the polymer, with values of 91.51 (6) and 91.88 (6)° for the larger angles, and 87.23 (6) and 87.25 (6)° for the smaller angles in **4epHgCl**. In the bromide analogue, **4epHgBr**, the two opposite angles *X*1—Hg—*X*1 and *X*2—Hg—*X*2 are 91.23 (2) and 89.09 (2)°, respectively, while the angles inside the polymer, *X*1—Hg—*X*2, are 89.34 (2) and 86.96 (2)°. The *X*2—Hg—*X*2 angle is 94.841 (18)° and the *X*1—Hg—*X*2 angle is 96.216 (19)° in **4epHgI**, with a semi-coordinated Hg···I interaction of 3.8988 (8) Å. The Hg—*X*—Hg angles are 91.51 (6) and 91.88 (6)° in **4epHgCl**, 91.23 (2) and 89.09 (2)° in **4epHgBr**, and 94.841 (18)° in **4epHgI.** As the size of the halide ligand increases, the interstrand *X*···*X* distances also increase from 3.792 (3) Å in

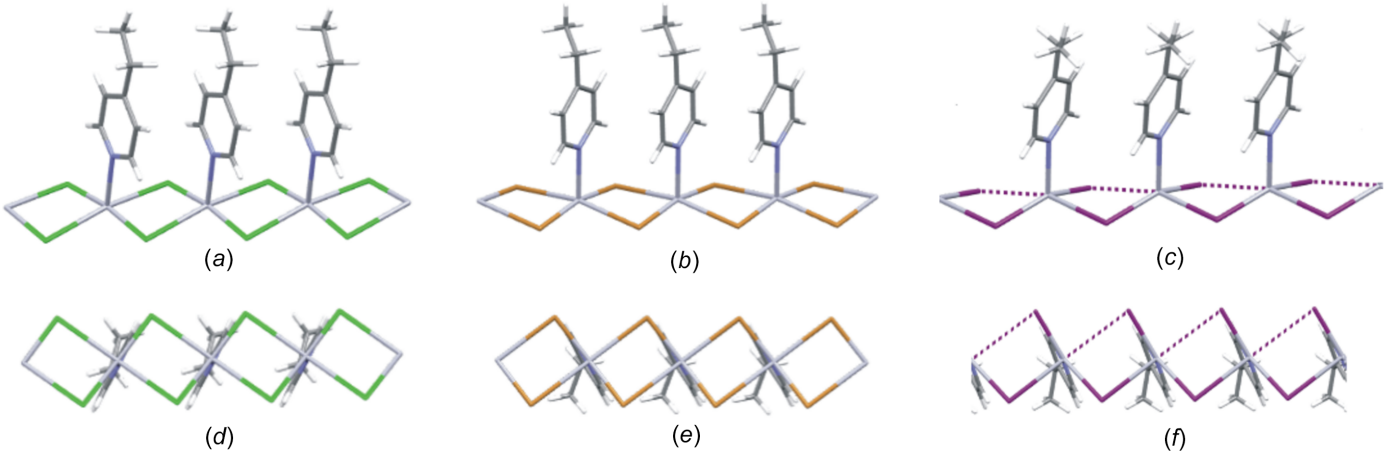

Figure 2
The halide-bibridged polymer chains in (*a*) **4epHgCl**, (*b*) **4epHgBr** and (*c*) **4epHgI**. The pseudo-parallelogram inorganic portion and the organic ligand tilt in (*d*) **4epHgCl** and (*e*) **4epHgBr**, and (*f*) the inorganic portion and organic ligand tilt in **4epHgI**. The dotted lines in parts (*c*) and (*f*) indicate longer and weaker Hg···I bonding interaction in the polymeric structure.

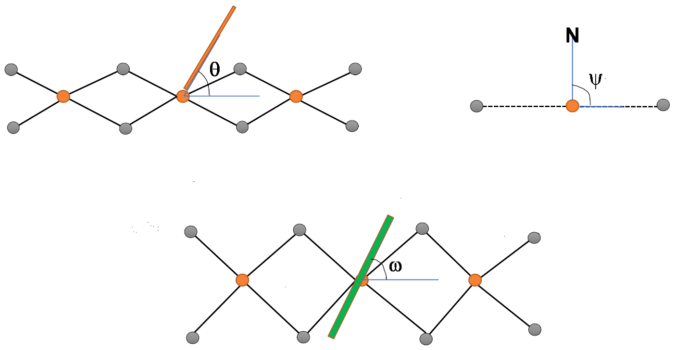

Figure 3
The descriptor angles θ, ψ and ω adapted from Hu *et al.* (2003). The orange spheres represent the metal cations, the grey spheres represent the bridging halide ligands and the thick orange and green lines represent the plane that contains the aromatic ring.

4epHgCl to 3.998 (1) Å in **4epHgBr** to 4.3503 (9) Å in **4epHgI**. This difference might be the reason for the formation of a less-symmetric structure as the size of the bridging halide increases (Hu *et al.*, 2007).

While the aromatic groups of the ligands are coplanar in all the structures, the one-dimensional polymers differ in terms of the relative orientation of their methyl substituents, as illustrated in Figs. Figs. 2(*d*)–(*f*). This difference in orientation is also evidenced by the C2—C3—C6—C7 and C4—C3—C6—C7 torsion angles of 170.2 (7) and −12.1 (12)° in **4epHgCl**, −130.2 (9) and 50.0 (12)° in **4epHgBr** and −147.0 (12) and 32.1 (19)° in **4epHgI**. Furthermore, the perpendicular distance between the plane containing the aromatic ring and the terminal aliphatic C7 atom increases from 0.262 Å in **4epHgCl** to 1.078 Å in **4epHgBr**; however, this distance decreases to 0.766 Å in **4epHgI**, indicating that the spatial orientation of the ethyl group of the organic ligand is influenced by the size of the halide ligand in the polymeric chain.

In order to compare the geometric features of the one-dimensional halide-bibridged polymers for systems with composition $[Hg(\mu\text{-}X)_2(L)_2]_n$, the structural descriptor angles θ, ψ and ω, originally defined by Hu *et al.* (2003), are used in this study, with small modifications made to the descriptors, as explained below. The descriptors are shown in Fig. 3. The angle θ indicates the orientation of the organic N-donor ligand relative to the one-dimensional halide-bridged chain, while the angle ψ is defined as the angle between the N atom, the metal ion to which it is coordinated and the adjacent metal centre (N—M1$\cdots$$M$2). The angle, ω, between the aromatic ring plane and the metal centre plane that passes through the Hg metal centres of equivalent halide-bridged polymers gives an indication of the degree of tilt of the aromatic group of the organic ligand relative to the halide-bridged polymer, as

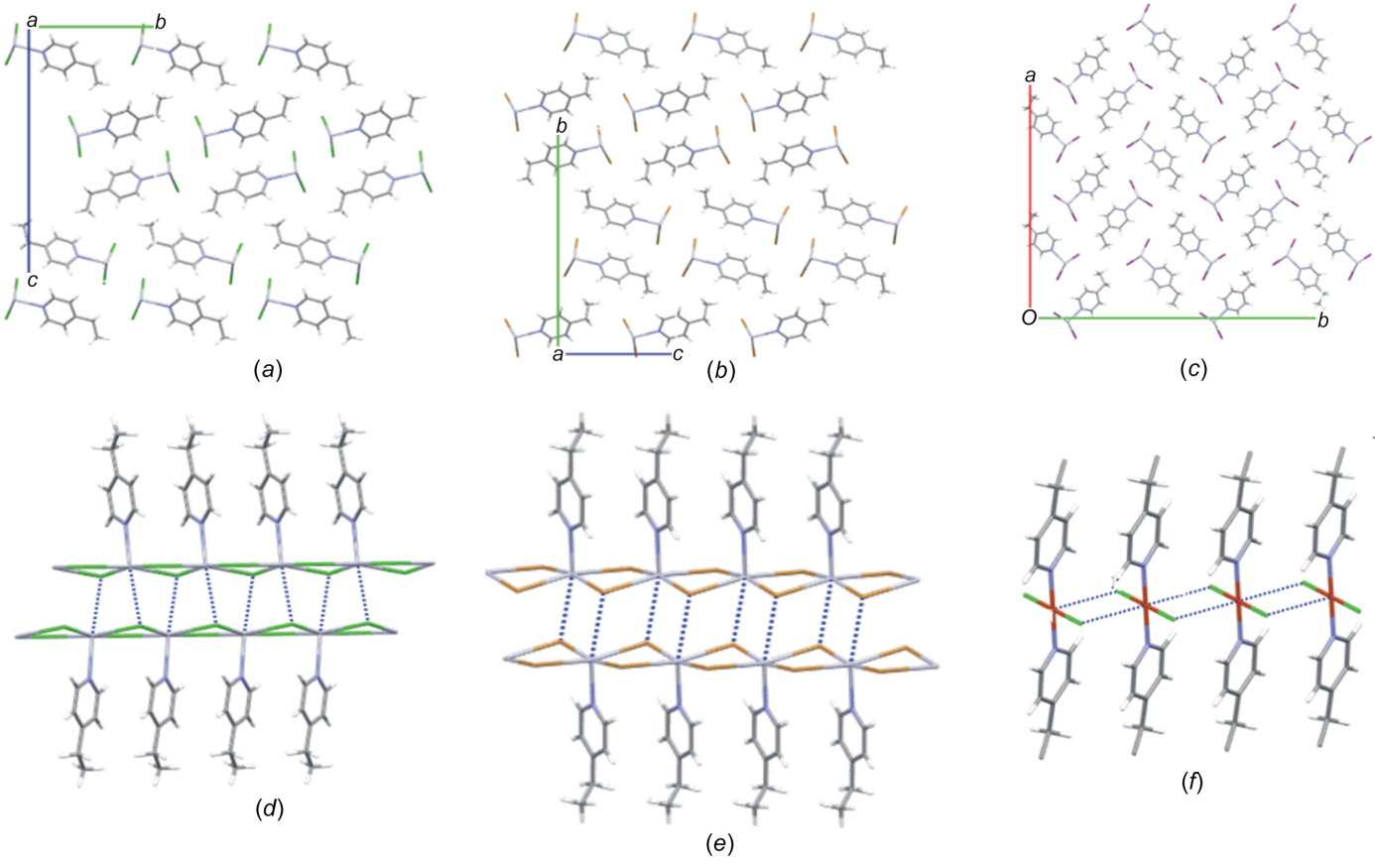

Figure 4
Packing diagrams of (*a*) **4epHgCl**, (*b*) **4epHgBr** and (*c*) **4epHgI**. The long semi-coordinated interactions forming the pseudo-octahedral polymer in (*d*) **4epHgCl** and (*e*) **4epHgBr**. (*f*) The halide-bibridged polymer in **4epCuBr** (CSD refcode CEPYCU; Laing *et al.*, 1971).

shown in Figs. 2(*d*) and 2(*e*). The schematic representation of the relative orientation of the aromatic ligand with respect to the halide-bridged polymer, represented by θ, ψ and ω, are shown in Fig. 3.

The angle between the aromatic plane of the organic ligand and the plane through the halide ligands, θ, is 80.96° in **4epHgCl**, 89.40° in **4epHgBr** and 75.74° in **4epHgI**. The structures of **4epHgCl**, **4epHgBr** and **4epHgI** exhibit ω angles of 65.31, 60.01 and 66.67°, respectively. There is a slight decrease in the ω angle from **4epHgCl** to **4epHgBr**, indicating that there is a larger degree of organic ligand rotation with the increase in size of the halide ligand. When the halide ligand changes to iodide, this trend does not continue, since a different structure is formed, as shown in Fig. 2(*f*), indicating that the size of the halide ligand in the halide-bridged polymer affects the conformation and rigidity of the polymer chain and this influences the orientation of the organic ligand attached to the chain. As the size of the halide ligand increases from chloride to iodide, the angle between the two metal-centre planes, containing the Hg^{II} cation, *X*1 and *X*2 in adjacent pseudo-parallelogram units, increases significantly from 15.60° in **4epHgCl** to 19.82° in **4epHgBr** to 30.50° in **4epHgI**, indicating increasing spatial distortion and flexibility of the Hg—*X*—Hg bridge.

The centroid-to-centroid distance between the pyridine moieties of the organic ligands is 3.938 Å in **4epHgCl**, 4.068 Å in **4epHgBr** and 4.325 Å in **4epHgI**, indicating weak aromatic interactions between neighbouring pyridine rings (Janiak *et al.*, 2000). It should be noted that the centroid-to-centroid distance depends on the halide-bridge lengths. As the size of the halide ligand increases from chloride to bromide to iodide, both the Hg—*X* and the Hg···Hg distances increase, causing an increase in the centroid-to-centroid distances between the pyridine moieties of the organic ligands. The ψ angle is 85.9 (1)° for **4epHgCl**, 88.0 (2)° for **4epHgBr** and 83.1 (2)° for **4epHgI**. The observed values of the ψ and θ angles in these halide-bibridged polymers indicate that the organic ligands are not perpendicular to the inorganic plane. This orientation has been adopted to ensure stability of the polymer *via* weak C—H···*X* hydrogen-bonding interactions, as listed in Table S2 in the supporting information. As can be seen from Table S2, both the donor–acceptor (*D*···*A*) distances and *D*—H···*A* angles increase as the size of the halide ligand increases. This results in weaker hydrogen-bonding interactions as the size of the halide increases and hence looser molecular packing of the polymeric chains within the crystal lattice.

The packing diagrams are illustrated in Figs. 4(*a*)–(*c*). Pairs of the halide-bridged polymers pack in a head-to-tail fashion, forming a layered structure in **4epHgCl** and **4epHgBr**, and a checkerboard pattern in **4epHgI**. The one-dimensional halide-bibridged polymers in the structures of **4epHgCl** and **4epHgBr** pack in such a way that the halide-bridged portions of two neighbouring polymeric chains approach each other, as shown in Figs. 4(*d*) and 4(*e*). This allows for the formation of long semi-coordinated Hg···*X*···Hg interactions to neighbouring polymer chains, as illustrated in Figs. 4(*d*) and 4(*e*), resulting in a pseudo-one-dimensional halide-bridged polymer that shows octahedral coordination of the Hg^{II} ions, which completes the coordination of the Hg^{II} ion. The Hg···*X* contact distances are 3.394 (2) Å in **4epHgCl** and 3.5909 (9) Å in **4epHgBr**, indicating that the Hg···*X* interactions between neighbouring polymer chains become weaker as the size of the halide ligand increases from chloride to bromide. This type of interchain interaction between polymers of this type is also seen in the structure comprised of $HgBr_2$ and phenazine organic ligands (Slabbert *et al.*, 2015*b*). The packing arrangement in **4epHgI** is different to that of **4epHgCl** and **4epHgBr**, with adjacent polymer chain pairs rotated 90° relative to each other and with no interchain Hg···I interactions between neighbouring polymer chains. This means that the change of the halide ligand from chloride to bromide, with the organic ligand and metal ion remaining constant, can be accommodated in the specific structural type; however, the change to the larger iodide ligand represents a tipping point that requires a change to a different structure type.

The $CuBr_2$ analogue of **4epCuBr** has been reported (CSD refcode CEPYCU; Laing *et al.*, 1971); however, this compound exhibits a halide-bibridged polymer with a flat metal–halide portion, in which the Cu^{II} ion displays a tetragonal geometry due to Jahn–Teller distortion, with the 4-Etpy organic ligand coordinating to both sides of the halide-bibridged polymer, as illustrated in Fig. 4(*f*).

4. Conclusions

4epHgCl, **4epHgBr** and **4epHgI** display similar one-dimensional scalloped halide-bridged polymeric structures involving two halide ligands bridging two metal centres, in which the Hg^{II} ion adopts a coordination number of five. The size of the halide ligand has a significant effect on the structure, geometry and packing arrangement of the polymer chains, with **4epHgI** displaying a different packing motif compared to the chloride and bromide analogues. In the structures of **4epHgCl** and **4epHgBr**, the polymer chains further associate *via* long semi-coordinated Hg···*X* interactions to form a pseudo-octahedral polymer. As the size of the halide ligands increases, the Hg—*X* bond length within the polymer chain increases, causing structural distortion in the polymer chain. The change of the halide ligand to the larger iodide ligand disrupts the formation of the regular halide-bibridged polymeric chain observed in the chloride and bromide analogues, with **4epHgI** displaying pseudo-bridging in the polymer chain.

Acknowledgements

The author would like to thank Dr F. Malan for assistance with the collection of the crystallographic data. BMPB-B acknowledges funding from the University of Pretoria as part of the RDP programme.

Conflict of interest

There are no conflicts of interest.

References

Bruker (2013). *APEX2*, *SAINT-Plus* and *SADABS*. Bruker AXS Inc., Madison, Wisconsin, USA.

Canty, A. J., Raston, C. L., Skelton, B. W. & White, A. H. (1982). *J. Chem. Soc. Dalton Trans.* pp. 15–18.

Crawford, V. H. & Hatfield, W. E. (1977). *Inorg. Chem.* **16**, 1336–1341.

Doerrer, L. H. (2010). *Dalton Trans.* **39**, 3543–3553.

Dolomanov, O. V., Bourhis, L. J., Gildea, R. J., Howard, J. A. K. & Puschmann, H. (2009). *J. Appl. Cryst.* **42**, 339–341.

Eckberg, R. P. & Hatfield, W. E. (1975). *J. Chem. Soc. Dalton Trans.* pp. 616–620.

Englert, U. (2010). *Coord. Chem. Rev.* **254**, 537–554.

Estes, W. E., Gavel, D. P., Hatfield, W. E. & Hodgson, D. J. (1978). *Inorg. Chem.* **17**, 1415–1421.

Farrugia, L. J. (2012). *J. Appl. Cryst.* **45**, 849–854.

Givaja, G., Amo-Ochoa, P., Gómez-García, C. J. & Zamora, F. (2012). *Chem. Soc. Rev.* **41**, 115–147.

Groom, C. R., Bruno, I. J., Lightfoot, M. P. & Ward, S. C. (2016). *Acta Cryst.* B**72**, 171–179.

Hu, C. & Englert, U. (2001). *CrystEngComm* **23**, 1–5.

Hu, C., Kalf, I. & Englert, U. (2007). *CrystEngComm* **9**, 603–610.

Hu, C., Li, Q. & Englert, U. (2003). *CrystEngComm* **5**, 519–529.

Janiak, C. (2000). *J. Chem. Soc. Dalton Trans.* pp. 3885–3896.

Kumar, M., Dalela, S. & Dinesh, S. (2013). *AIP Conf. Proc.* pp. 771–772.

Laing, M. & Carr, G. (1971). *J. Chem. Soc. A* pp. 1141–1144.

Macrae, C. F., Sovago, I., Cottrell, S. J., Galek, P. T. A., McCabe, P., Pidcock, E., Platings, M., Shields, G. P., Stevens, J. S., Towler, M. & Wood, P. A. (2020). *J. Appl. Cryst.* **53**, 226–235.

Mahmoudi, G. & Morsali, A. (2009). *CrystEngComm* **11**, 1868–1879.

Mobin, S. M., Srivastava, A. K., Mathur, P. & Lahiri, G. K. (2010). *Dalton Trans.* **39**, 8698–8705.

Morsali, A. & Masoomi, M. Y. (2009). *Coord. Chem. Rev.* **253**, 1882–1905.

Sheldrick, G. M. (2015*a*). *Acta Cryst.* A**71**, 3–8.

Sheldrick, G. M. (2015*b*). *Acta Cryst.* C**71**, 3–8.

Slabbert, C. & Rademeyer, M. (2015*a*). *Coord. Chem. Rev.* **288**, 18–49.

Slabbert, C. & Rademeyer, M. (2015*b*). *CrystEngComm* **17**, 9070–9096.

Spek, A. L. (2020). *Acta Cryst.* E**76**, 1–11.

Wang, R., Lehmann, C. W. & Englert, U. (2009). *Acta Cryst.* B**65**, 600–611.

Wei, M., Willett, R. D., Teske, D., Subbaraman, K. & Drumheller, J. E. (1996). *Inorg. Chem.* **35**, 5781–5785.

Zhang, W., Jeitler, J. R., Turnbull, M. M., Landee, C. P., Wei, M. & Willett, R. D. (1997). *Inorg. Chim. Acta* **256**, 183–198.

supporting information

Acta Cryst. (2025). C**81**, 680-686 [https://doi.org/10.1107/S2053229625009702]

Effect of the size of halide ligands on the crystal structures of halide-bibridged polymers of HgX_2 with 4-ethylpyridine

B. M. Parveen Beebeejaun-Boodoo

Computing details

***catena*-Poly[[(4-ethylpyridine)mercury(II)]-di-μ-chlorido], (4epHgCl_updated)**

Crystal data

$[HgCl_2(C_7H_9N)]$
M_r = 378.64
Orthorhombic, $P2_12_12_1$
a = 3.9382 (5) Å
b = 10.3571 (15) Å
c = 22.758 (3) Å
V = 928.3 (2) Å^3
Z = 4
$F(000)$ = 688
D_x = 2.709 Mg m^{-3}
Mo $K\alpha$ radiation, λ = 0.71073 Å
Cell parameters from 9940 reflections
θ = 2.7–26.4°
μ = 17.09 mm^{-1}
T = 150 K
Rod, colourless
0.51 × 0.23 × 0.12 mm

Data collection

Bruker PHOTON 100 CMOS diffractometer
φ and ω scans
Absorption correction: multi-scan (SADABS; Bruker, 2013)
T_{min} = 0.068, T_{max} = 0.260
16644 measured reflections
1876 independent reflections
1869 reflections with $I > 2\sigma(I)$
R_{int} = 0.058
θ_{max} = 26.4°, θ_{min} = 2.2°
h = −4→4
k = −12→12
l = −28→28

Refinement

Refinement on F^2
Least-squares matrix: full
$R[F^2 > 2\sigma(F^2)]$ = 0.020
$wR(F^2)$ = 0.053
S = 1.11
1876 reflections
103 parameters
0 restraints
Primary atom site location: iterative
Hydrogen site location: inferred from neighbouring sites
H-atom parameters constrained
$w = 1/[\sigma^2(F_o^2) + (0.0173P)^2 + 3.720P]$ where $P = (F_o^2 + 2F_c^2)/3$
$(\Delta/\sigma)_{max}$ = 0.003
$\Delta\rho_{max}$ = 1.29 e Å^{-3}
$\Delta\rho_{min}$ = −1.22 e Å^{-3}
Extinction correction: SHELXL, $Fc^*=kFc[1+0.001xFc^2\lambda^3/\sin(2\theta)]^{-1/4}$
Extinction coefficient: 0.0084 (5)
Absolute structure: Refined as an inversion twin.
Absolute structure parameter: 0.186 (14)

Special details

Geometry. All esds (except the esd in the dihedral angle between two l.s. planes) are estimated using the full covariance matrix. The cell esds are taken into account individually in the estimation of esds in distances, angles and torsion angles; correlations between esds in cell parameters are only used when they are defined by crystal symmetry. An approximate (isotropic) treatment of cell esds is used for estimating esds involving l.s. planes.

Refinement. Refined as a 2-component inversion twin.

All the single-crystal X-ray diffraction data were collected on a Bruker Venture diffractometer, with a Photon 100 CMOS detector, at 150 (2) K employing a combination of φ and ω scans. A monochromatic Mo $K\alpha$ radiation of wavelength 0.71073 Å, from an Iμs source, was employed as the irradiation source. Cooling was achieved using an Oxford Cryogenics Cryostream 700 cryostat. Data reduction were performed using the software *SAINT-Plus* (Bruker, 2013) and absorption corrections were performed using *SADABS* (Bruker, 2013) as part of the *APEX2* suite (Bruker, 2013). All the crystal structures were solved either by direct methods or intrinsic phasing using *SHELXT* (Sheldrick, 2015*a*), as part of the *WinGX* suite (Farrugia, 2012) and *OLEX2* (Dolomanov *et al.*, 2009). The structures were refined using *SHELXL2013* (Sheldrick, 2015*b*) in *WinGX* (Farrugia, 2012) and *OLEX2* (Dolomanov *et al.*, 2009) as GUI. Graphics and publication material were generated using *Mercury* (Macrae *et al.*, 2020) and *PLATON* (Spek, 2020).

Fractional atomic coordinates and isotropic or equivalent isotropic displacement parameters (Å²)

	x	*y*	*z*	U_{iso}*/U_{eq}
Hg1	0.23073 (7)	1.11285 (2)	0.57199 (2)	0.01796 (13)
N1	0.2748 (16)	0.8857 (5)	0.5996 (3)	0.0175 (12)
C5	0.1627 (19)	0.8454 (8)	0.6511 (3)	0.0196 (16)
H5	0.0456	0.9053	0.6754	0.023*
Cl1	0.6011 (5)	1.09430 (18)	0.49111 (8)	0.0196 (4)
C4	0.206 (2)	0.7210 (7)	0.6717 (3)	0.0191 (15)
H4	0.1194	0.6967	0.7090	0.023*
Cl2	−0.1398 (5)	1.17977 (19)	0.64681 (8)	0.0221 (4)
C3	0.3772 (19)	0.6323 (7)	0.6374 (3)	0.0154 (14)
C2	0.489 (2)	0.6735 (7)	0.5824 (3)	0.0181 (15)
H2	0.5991	0.6147	0.5567	0.022*
C1	0.4394 (19)	0.8019 (7)	0.5654 (3)	0.0185 (15)
H1	0.5250	0.8301	0.5286	0.022*
C6	0.438 (2)	0.4932 (8)	0.6548 (3)	0.0202 (16)
H6A	0.6784	0.4719	0.6466	0.024*
H6B	0.2959	0.4374	0.6295	0.024*
C7	0.364 (2)	0.4598 (8)	0.7185 (4)	0.0285 (19)
H7A	0.4304	0.3701	0.7260	0.043*
H7B	0.1211	0.4703	0.7262	0.043*
H7C	0.4939	0.5173	0.7443	0.043*

Atomic displacement parameters (Å²)

	U^{11}	U^{22}	U^{33}	U^{12}	U^{13}	U^{23}
Hg1	0.01893 (18)	0.01697 (18)	0.01797 (18)	0.00154 (13)	0.00375 (12)	−0.00102 (9)
N1	0.020 (3)	0.015 (3)	0.018 (3)	0.001 (4)	−0.002 (2)	−0.003 (2)
C5	0.023 (4)	0.021 (4)	0.016 (3)	0.002 (3)	0.001 (3)	−0.002 (3)
Cl1	0.0217 (9)	0.0194 (9)	0.0177 (8)	−0.0003 (7)	0.0046 (6)	−0.0005 (7)
C4	0.021 (4)	0.021 (3)	0.016 (3)	0.000 (3)	0.003 (3)	0.000 (3)
Cl2	0.0229 (10)	0.0223 (9)	0.0212 (9)	0.0024 (7)	0.0054 (7)	−0.0032 (7)

C3	0.018 (3)	0.016 (4)	0.013 (3)	−0.001 (3)	−0.004 (3)	0.005 (3)
C2	0.021 (4)	0.013 (4)	0.021 (4)	0.001 (3)	−0.002 (3)	−0.004 (3)
C1	0.023 (4)	0.019 (4)	0.013 (3)	−0.005 (3)	−0.004 (3)	−0.003 (3)
C6	0.027 (5)	0.018 (4)	0.015 (4)	0.002 (3)	0.000 (3)	0.001 (3)
C7	0.038 (5)	0.028 (4)	0.019 (4)	0.004 (4)	−0.003 (4)	0.010 (3)

Geometric parameters (Å, º)

Hg1—N1	2.441 (6)	C3—C6	1.514 (10)
Hg1—Cl1	2.3562 (18)	C2—H2	0.9500
Hg1—Cl2	2.3471 (18)	C2—C1	1.399 (11)
N1—C5	1.320 (9)	C1—H1	0.9500
N1—C1	1.334 (9)	C6—H6A	0.9900
C5—H5	0.9500	C6—H6B	0.9900
C5—C4	1.382 (11)	C6—C7	1.517 (10)
C4—H4	0.9500	C7—H7A	0.9800
C4—C3	1.380 (10)	C7—H7B	0.9800
C3—C2	1.393 (10)	C7—H7C	0.9800
Cl1—Hg1—N1	94.51 (15)	C1—C2—H2	120.2
Cl2—Hg1—N1	98.16 (15)	N1—C1—C2	121.7 (7)
Cl2—Hg1—Cl1	167.32 (7)	N1—C1—H1	119.1
C5—N1—Hg1	120.6 (5)	C2—C1—H1	119.1
C5—N1—C1	118.3 (6)	C3—C6—H6A	108.3
C1—N1—Hg1	120.8 (5)	C3—C6—H6B	108.3
N1—C5—H5	118.2	C3—C6—C7	115.9 (7)
N1—C5—C4	123.7 (7)	H6A—C6—H6B	107.4
C4—C5—H5	118.2	C7—C6—H6A	108.3
C5—C4—H4	120.4	C7—C6—H6B	108.3
C3—C4—C5	119.3 (7)	C6—C7—H7A	109.5
C3—C4—H4	120.4	C6—C7—H7B	109.5
C4—C3—C2	117.3 (7)	C6—C7—H7C	109.5
C4—C3—C6	124.2 (7)	H7A—C7—H7B	109.5
C2—C3—C6	118.4 (7)	H7A—C7—H7C	109.5
C3—C2—H2	120.2	H7B—C7—H7C	109.5
C3—C2—C1	119.7 (7)		
Hg1—N1—C5—C4	−174.1 (6)	C4—C3—C2—C1	2.8 (11)
Hg1—N1—C1—C2	175.2 (5)	C4—C3—C6—C7	−12.1 (12)
N1—C5—C4—C3	0.4 (12)	C3—C2—C1—N1	−2.6 (11)
C5—N1—C1—C2	1.1 (11)	C2—C3—C6—C7	170.2 (7)
C5—C4—C3—C2	−1.7 (11)	C1—N1—C5—C4	0.0 (11)
C5—C4—C3—C6	−179.4 (7)	C6—C3—C2—C1	−179.4 (7)

Hydrogen-bond geometry (Å, º)

D—H···*A*	*D*—H	H···*A*	*D*···*A*	*D*—H···*A*
C1—H1···Cl1	0.95	2.88	3.527 (8)	126

catena-Poly[[(4-ethylpyridine)mercury(II)]-di-μ-bromido] (4epHgBr_updated)

Crystal data

$[HgBr_2(C_7H_9N)]$
$M_r = 467.54$
Monoclinic, $P2_1/c$
$a = 4.0679$ (5) Å
$b = 22.583$ (3) Å
$c = 10.9050$ (14) Å
$\beta = 95.488$ (4)°
$V = 997.2$ (2) Å^3
$Z = 4$
$F(000) = 832$
$D_x = 3.114$ Mg m^{-3}
Mo $K\alpha$ radiation, $\lambda = 0.71073$ Å
Cell parameters from 9889 reflections
$\theta = 2.6$–$26.4°$
$\mu = 23.39$ mm^{-1}
$T = 150$ K
Rod, colourless
0.42 × 0.18 × 0.10 mm

Data collection

Bruker PHOTON 100 CMOS diffractometer
φ and ω scans
Absorption correction: multi-scan (SADABS; Bruker, 2013)
$T_{min} = 0.244$, $T_{max} = 0.745$
21065 measured reflections
2024 independent reflections
1908 reflections with $I > 2\sigma(I)$
$R_{int} = 0.062$
$\theta_{max} = 26.4°$, $\theta_{min} = 2.6°$
$h = -5 \rightarrow 5$
$k = -28 \rightarrow 28$
$l = -13 \rightarrow 13$

Refinement

Refinement on F^2
Least-squares matrix: full
$R[F^2 > 2\sigma(F^2)] = 0.033$
$wR(F^2) = 0.094$
$S = 1.08$
2024 reflections
96 parameters
0 restraints
Primary atom site location: iterative
Hydrogen site location: inferred from neighbouring sites
H-atom parameters constrained
$w = 1/[\sigma^2(F_o^2) + (0.054P)^2 + 11.1648P]$ where $P = (F_o^2 + 2F_c^2)/3$
$(\Delta/\sigma)_{max} = 0.001$
$\Delta\rho_{max} = 2.19$ e Å^{-3}
$\Delta\rho_{min} = -1.85$ e Å^{-3}
Extinction correction: SHELXL2013 (Sheldrick, 2015*b*), $Fc^* = kFc[1+0.001xFc^2\lambda^3/\sin(2\theta)]^{-1/4}$
Extinction coefficient: 0.0037 (4)

Special details

Geometry. All esds (except the esd in the dihedral angle between two l.s. planes) are estimated using the full covariance matrix. The cell esds are taken into account individually in the estimation of esds in distances, angles and torsion angles; correlations between esds in cell parameters are only used when they are defined by crystal symmetry. An approximate (isotropic) treatment of cell esds is used for estimating esds involving l.s. planes.

Refinement. All the single-crystal X-ray diffraction data were collected on a Bruker Venture diffractometer, with a Photon 100 CMOS detector, at 150 (2) K employing a combination of φ and ω scans. A monochromatic Mo $K\alpha$ radiation of wavelength 0.71073 Å, from an Iμs source, was employed as the irradiation source. Cooling was achieved using an Oxford Cryogenics Cryostream 700 cryostat. Data reduction were performed using the software *SAINT-Plus* (Bruker, 2013) and absorption corrections were performed using *SADABS* (Bruker, 2013) as part of the *APEX2* suite (Bruker, 2013). All the crystal structures were solved either by direct methods or intrinsic phasing using *SHELXT* (Sheldrick, 2015*a*), as part of the *WinGX* suite (Farrugia, 2012) and *OLEX2* (Dolomanov *et al.*, 2009). The structures were refined using *SHELXL2013* (Sheldrick, 2015*b*) in *WinGX* (Farrugia, 2012) and *OLEX2* (Dolomanov *et al.*, 2009) as GUI. Graphics and publication material were generated using *Mercury* (Macrae *et al.*, 2020) and *PLATON* (Spek, 2020).

Fractional atomic coordinates and isotropic or equivalent isotropic displacement parameters (Å^2)

	x	y	z	U_{iso}*/U_{eq}
Hg1	0.41038 (7)	0.42522 (2)	0.13824 (3)	0.01892 (16)

Br1	0.79830 (19)	0.51020 (3)	0.15997 (7)	0.0187 (2)
Br2	0.02711 (19)	0.34692 (3)	0.05465 (7)	0.0208 (2)
N1	0.4445 (17)	0.3968 (3)	0.3546 (6)	0.0194 (14)
C1	0.613 (2)	0.4299 (4)	0.4419 (8)	0.0224 (18)
H1	0.7134	0.4655	0.4179	0.027*
C2	0.645 (2)	0.4143 (4)	0.5656 (8)	0.0194 (16)
H2	0.7625	0.4393	0.6246	0.023*
C3	0.505 (2)	0.3618 (3)	0.6029 (7)	0.0179 (11)
C4	0.332 (2)	0.3280 (4)	0.5112 (7)	0.0221 (17)
H4	0.2344	0.2915	0.5316	0.027*
C5	0.303 (2)	0.3476 (3)	0.3901 (7)	0.0179 (11)
H5	0.1763	0.3247	0.3298	0.022*
C6	0.541 (2)	0.3436 (4)	0.7359 (7)	0.0251 (18)
H6A	0.3254	0.3483	0.7696	0.030*
H6B	0.6999	0.3707	0.7821	0.030*
C7	0.659 (2)	0.2804 (4)	0.7573 (8)	0.028 (2)
H7A	0.4999	0.2531	0.7144	0.042*
H7B	0.6791	0.2718	0.8458	0.042*
H7C	0.8749	0.2754	0.7255	0.042*

Atomic displacement parameters (Å²)

	U^{11}	U^{22}	U^{33}	U^{12}	U^{13}	U^{23}
Hg1	0.0196 (2)	0.0170 (2)	0.0195 (2)	−0.00505 (11)	−0.00147 (13)	−0.00051 (10)
Br1	0.0194 (4)	0.0140 (4)	0.0225 (4)	−0.0036 (3)	0.0012 (3)	−0.0016 (3)
Br2	0.0220 (4)	0.0159 (4)	0.0234 (4)	−0.0042 (3)	−0.0036 (3)	−0.0022 (3)
N1	0.020 (3)	0.018 (4)	0.020 (3)	0.002 (3)	−0.002 (3)	−0.006 (3)
C1	0.029 (5)	0.017 (4)	0.021 (4)	−0.006 (3)	−0.001 (3)	0.001 (3)
C2	0.014 (4)	0.018 (4)	0.025 (4)	−0.002 (3)	−0.004 (3)	−0.001 (3)
C3	0.024 (3)	0.011 (3)	0.018 (3)	−0.003 (2)	−0.002 (2)	0.000 (2)
C4	0.030 (4)	0.018 (4)	0.018 (4)	−0.001 (3)	0.002 (3)	0.002 (3)
C5	0.024 (3)	0.011 (3)	0.018 (3)	−0.003 (2)	−0.002 (2)	0.000 (2)
C6	0.036 (5)	0.026 (5)	0.012 (4)	−0.002 (4)	−0.004 (3)	−0.001 (3)
C7	0.042 (5)	0.013 (4)	0.027 (5)	−0.003 (4)	−0.006 (4)	0.003 (3)

Geometric parameters (Å, º)

Hg1—Br1	2.4815 (8)	C3—C6	1.501 (11)
Hg1—Br2	2.4732 (8)	C4—H4	0.9500
Hg1—N1	2.436 (7)	C4—C5	1.387 (11)
N1—C1	1.346 (10)	C5—H5	0.9500
N1—C5	1.325 (11)	C6—H6A	0.9900
C1—H1	0.9500	C6—H6B	0.9900
C1—C2	1.388 (12)	C6—C7	1.517 (12)
C2—H2	0.9500	C7—H7A	0.9800
C2—C3	1.393 (11)	C7—H7B	0.9800
C3—C4	1.395 (11)	C7—H7C	0.9800

Br2—Hg1—Br1	163.92 (3)	C5—C4—H4	120.0
N1—Hg1—Br1	97.73 (16)	N1—C5—C4	123.1 (7)
N1—Hg1—Br2	98.28 (16)	N1—C5—H5	118.4
C1—N1—Hg1	121.1 (6)	C4—C5—H5	118.4
C5—N1—Hg1	121.2 (5)	C3—C6—H6A	108.8
C5—N1—C1	117.7 (7)	C3—C6—H6B	108.8
N1—C1—H1	118.6	C3—C6—C7	114.0 (7)
N1—C1—C2	122.7 (8)	H6A—C6—H6B	107.7
C2—C1—H1	118.6	C7—C6—H6A	108.8
C1—C2—H2	120.1	C7—C6—H6B	108.8
C1—C2—C3	119.8 (8)	C6—C7—H7A	109.5
C3—C2—H2	120.1	C6—C7—H7B	109.5
C2—C3—C4	116.7 (7)	C6—C7—H7C	109.5
C2—C3—C6	120.7 (7)	H7A—C7—H7B	109.5
C4—C3—C6	122.6 (7)	H7A—C7—H7C	109.5
C3—C4—H4	120.0	H7B—C7—H7C	109.5
C5—C4—C3	119.9 (8)		

Hg1—N1—C1—C2	−178.2 (6)	C2—C3—C4—C5	−0.8 (12)
Hg1—N1—C5—C4	176.2 (6)	C2—C3—C6—C7	−130.2 (9)
N1—C1—C2—C3	1.2 (13)	C3—C4—C5—N1	2.7 (13)
C1—N1—C5—C4	−2.6 (12)	C4—C3—C6—C7	50.0 (12)
C1—C2—C3—C4	−1.1 (12)	C5—N1—C1—C2	0.6 (13)
C1—C2—C3—C6	179.1 (8)	C6—C3—C4—C5	179.0 (8)

Hydrogen-bond geometry (Å, º)

D—H···*A*	*D*—H	H···*A*	*D*···*A*	*D*—H···*A*
C1—H1···Br1	0.95	3.04	3.708 (9)	129
C2—H2···Br1^{i}	0.95	3.03	3.961 (8)	166
C5—H5···Br2	0.95	3.04	3.723 (8)	130

Symmetry code: (i) −*x*+2, −*y*+1, −*z*+1.

catena-Poly[[(4-ethylpyridine)mercury(II)]-di-μ-iodido] (4epHgI_updated)

Crystal data

[$HgI_2(C_7H_9N)$]
M_r = 561.54
Orthorhombic, *Fdd*2
a = 30.3836 (14) Å
b = 34.6159 (16) Å
c = 4.3247 (2) Å
V = 4548.5 (4) Å^3
Z = 16
F(000) = 3904

D_x = 3.280 Mg m^{-3}
Mo *K*α radiation, λ = 0.71073 Å
Cell parameters from 9539 reflections
θ = 2.4–35.2°
μ = 18.91 mm^{-1}
T = 150 K
Needle, colourless
0.23 × 0.06 × 0.06 mm

Data collection

Bruker PHOTON 100 CMOS diffractometer
φ and ω scans
Absorption correction: multi-scan (SADABS; Bruker, 2013)
T_{min} = 0.366, T_{max} = 0.747
30677 measured reflections
2271 independent reflections
2251 reflections with $I > 2\sigma(I)$
R_{int} = 0.038
θ_{max} = 26.4°, θ_{min} = 2.4°
h = −37→37
k = −42→42
l = −5→5

Refinement

Refinement on F^2
Least-squares matrix: full
$R[F^2 > 2\sigma(F^2)]$ = 0.018
$wR(F^2)$ = 0.045
S = 1.15
2271 reflections
102 parameters
1 restraint
Primary atom site location: iterative
Hydrogen site location: inferred from neighbouring sites
H-atom parameters constrained
$w = 1/[\sigma^2(F_o^2) + (0.0183P)^2 + 39.4372P]$ where $P = (F_o^2 + 2F_c^2)/3$
$(\Delta/\sigma)_{max}$ = 0.001
$\Delta\rho_{max}$ = 1.17 e Å^{-3}
$\Delta\rho_{min}$ = −0.46 e Å^{-3}
Absolute structure: Refined as an inversion twin.
Absolute structure parameter: 0.026 (7)

Special details

Geometry. All esds (except the esd in the dihedral angle between two l.s. planes) are estimated using the full covariance matrix. The cell esds are taken into account individually in the estimation of esds in distances, angles and torsion angles; correlations between esds in cell parameters are only used when they are defined by crystal symmetry. An approximate (isotropic) treatment of cell esds is used for estimating esds involving l.s. planes.

Refinement. Refined as a 2-component inversion twin.
All the single-crystal X-ray diffraction data were collected on a Bruker Venture diffractometer, with a Photon 100 CMOS detector, at 150 (2) K employing a combination of φ and ω scans. A monochromatic Mo $K\alpha$ radiation of wavelength 0.71073 Å, from an Iμs source, was employed as the irradiation source. Cooling was achieved using an Oxford Cryogenics Cryostream 700 cryostat. Data reduction were performed using the software *SAINT-Plus* (Bruker, 2013) and absorption corrections were performed using *SADABS* (Bruker, 2013) as part of the *APEX2* suite (Bruker, 2013). All the crystal structures were solved either by direct methods or intrinsic phasing using *SHELXT* (Sheldrick, 2015*a*), as part of the *WinGX* suite (Farrugia, 2012) and *OLEX2* (Dolomanov *et al.*, 2009). The structures were refined using *SHELXL2013* (Sheldrick, 2015*b*) in *WinGX* (Farrugia, 2012) and *OLEX2* (Dolomanov *et al.*, 2009) as GUI. Graphics and publication material were generated using *Mercury* (Macrae *et al.*, 2020) and *PLATON* (Spek, 2020).

Fractional atomic coordinates and isotropic or equivalent isotropic displacement parameters (Å^2)

	x	y	z	U_{iso}*/U_{eq}
Hg1	0.23465 (2)	0.12095 (2)	0.53653 (8)	0.02757 (9)
I2	0.27181 (2)	0.16710 (2)	0.12059 (11)	0.02746 (13)
I1	0.16471 (2)	0.09297 (2)	0.81462 (14)	0.03344 (13)
N1	0.2905 (2)	0.07371 (19)	0.6022 (18)	0.0300 (15)
C5	0.3319 (3)	0.0819 (2)	0.525 (3)	0.039 (2)
H5	0.3379	0.1060	0.4280	0.047*
C4	0.3664 (3)	0.0569 (2)	0.580 (3)	0.041 (2)
H4	0.3953	0.0637	0.5165	0.049*
C3	0.3590 (3)	0.0219 (2)	0.726 (2)	0.035 (2)
C2	0.3160 (3)	0.0136 (2)	0.805 (3)	0.038 (2)
H2	0.3090	−0.0103	0.8999	0.046*

C1	0.2830 (3)	0.0402 (2)	0.746 (2)	0.036 (2)
H1	0.2538	0.0344	0.8101	0.044*
C6	0.3953 (3)	−0.0061 (3)	0.802 (4)	0.056 (3)
H6A	0.3858	−0.0219	0.9809	0.067*
H6B	0.3990	−0.0238	0.6243	0.067*
C7	0.4380 (3)	0.0106 (3)	0.875 (3)	0.058 (3)
H7A	0.4507	0.0222	0.6877	0.087*
H7B	0.4577	−0.0096	0.9516	0.087*
H7C	0.4345	0.0306	1.0335	0.087*

Atomic displacement parameters (Å²)

	U^{11}	U^{22}	U^{33}	U^{12}	U^{13}	U^{23}
Hg1	0.02800 (14)	0.02640 (14)	0.02831 (16)	0.00299 (12)	0.00808 (12)	0.00549 (13)
I2	0.0359 (3)	0.0274 (3)	0.0191 (2)	−0.0078 (2)	0.0003 (2)	0.00268 (18)
I1	0.0311 (2)	0.0400 (3)	0.0292 (3)	−0.0081 (2)	0.0101 (2)	−0.0027 (2)
N1	0.032 (3)	0.025 (3)	0.033 (4)	0.001 (3)	0.003 (3)	0.004 (3)
C5	0.030 (4)	0.028 (4)	0.059 (6)	−0.001 (3)	0.017 (4)	0.007 (5)
C4	0.025 (4)	0.029 (4)	0.070 (7)	0.001 (3)	0.005 (5)	−0.001 (5)
C3	0.030 (4)	0.027 (4)	0.047 (6)	0.002 (3)	−0.009 (4)	−0.001 (4)
C2	0.032 (4)	0.024 (4)	0.058 (6)	−0.002 (3)	−0.010 (5)	0.010 (5)
C1	0.031 (4)	0.030 (4)	0.049 (5)	−0.001 (3)	0.004 (4)	0.010 (4)
C6	0.033 (4)	0.030 (5)	0.106 (10)	0.005 (4)	−0.017 (7)	0.004 (6)
C7	0.044 (5)	0.038 (5)	0.092 (10)	−0.004 (4)	−0.026 (6)	0.008 (6)

Geometric parameters (Å, º)

Hg1—I2^{i}	3.1949 (6)	C3—C2	1.381 (13)
Hg1—I2	2.6576 (6)	C3—C6	1.504 (13)
Hg1—I1	2.6269 (6)	C2—H2	0.9500
Hg1—N1	2.373 (7)	C2—C1	1.384 (12)
I2—Hg1^{ii}	3.1949 (6)	C1—H1	0.9500
N1—C5	1.332 (10)	C6—H6A	0.9900
N1—C1	1.335 (11)	C6—H6B	0.9900
C5—H5	0.9500	C6—C7	1.455 (13)
C5—C4	1.381 (12)	C7—H7A	0.9800
C4—H4	0.9500	C7—H7B	0.9800
C4—C3	1.385 (13)	C7—H7C	0.9800
I2—Hg1—I2^{i}	94.841 (18)	C3—C2—H2	119.9
I1—Hg1—I2^{i}	96.216 (19)	C3—C2—C1	120.2 (8)
I1—Hg1—I2	151.07 (2)	C1—C2—H2	119.9
N1—Hg1—I2	101.05 (17)	N1—C1—C2	122.7 (8)
N1—Hg1—I2^{i}	89.85 (18)	N1—C1—H1	118.7
N1—Hg1—I1	105.63 (17)	C2—C1—H1	118.7
Hg1—I2—Hg1^{ii}	94.841 (18)	C3—C6—H6A	108.2
C5—N1—Hg1	119.8 (6)	C3—C6—H6B	108.2
C5—N1—C1	117.6 (7)	H6A—C6—H6B	107.3

C1—N1—Hg1	122.2 (5)	C7—C6—C3	116.5 (8)
N1—C5—H5	118.7	C7—C6—H6A	108.2
N1—C5—C4	122.6 (8)	C7—C6—H6B	108.2
C4—C5—H5	118.7	C6—C7—H7A	109.5
C5—C4—H4	119.8	C6—C7—H7B	109.5
C5—C4—C3	120.4 (8)	C6—C7—H7C	109.5
C3—C4—H4	119.8	H7A—C7—H7B	109.5
C4—C3—C6	123.0 (9)	H7A—C7—H7C	109.5
C2—C3—C4	116.5 (8)	H7B—C7—H7C	109.5
C2—C3—C6	120.5 (9)		

Hg1—N1—C5—C4	174.8 (9)	C4—C3—C2—C1	−1.9 (15)
Hg1—N1—C1—C2	−175.3 (8)	C4—C3—C6—C7	32.1 (19)
N1—C5—C4—C3	−1.3 (18)	C3—C2—C1—N1	2.6 (16)
C5—N1—C1—C2	−2.5 (15)	C2—C3—C6—C7	−147.0 (12)
C5—C4—C3—C2	1.3 (16)	C1—N1—C5—C4	1.9 (16)
C5—C4—C3—C6	−177.8 (12)	C6—C3—C2—C1	177.2 (11)

Symmetry codes: (i) *x*, *y*, *z*+1; (ii) *x*, *y*, *z*−1.

Hydrogen-bond geometry (Å, º)

D—H···*A*	*D*—H	H···*A*	*D*···*A*	*D*—H···*A*
C5—H5···I2	0.95	3.21	3.883 (9)	130
C5—H5···I1^{iii}	0.95	3.32	4.130 (9)	144

Symmetry code: (iii) *x*+1/4, −*y*+1/4, *z*−3/4.